Deep Scatter Estimation for Coarse Anti-Scatter Grids as used in Photon-Counting CT

Julien Erath[1,2,3], Jan Magonov[1,2,3], Joscha Maier[1], Eric Fournié [2], Martin Petersilka[2], Karl Stierstorfer[2], and Marc Kachelrieß[1,3]

[1]German Cancer Research Center (DKFZ), Heidelberg, Germany

[2]Siemens Healthineers, Forchheim, Germany

[3]Ruprecht-Karls-Universität, Heidelberg, Germany

www.dkfz.de/ct

SIEMENS Healthineers

dkfz. DEUTSCHES KREBSFORSCHUNGSZENTRUM IN DER HELMHOLTZ-GEMEINSCHAFT

Photon-Counting enables Visualization of Small Details

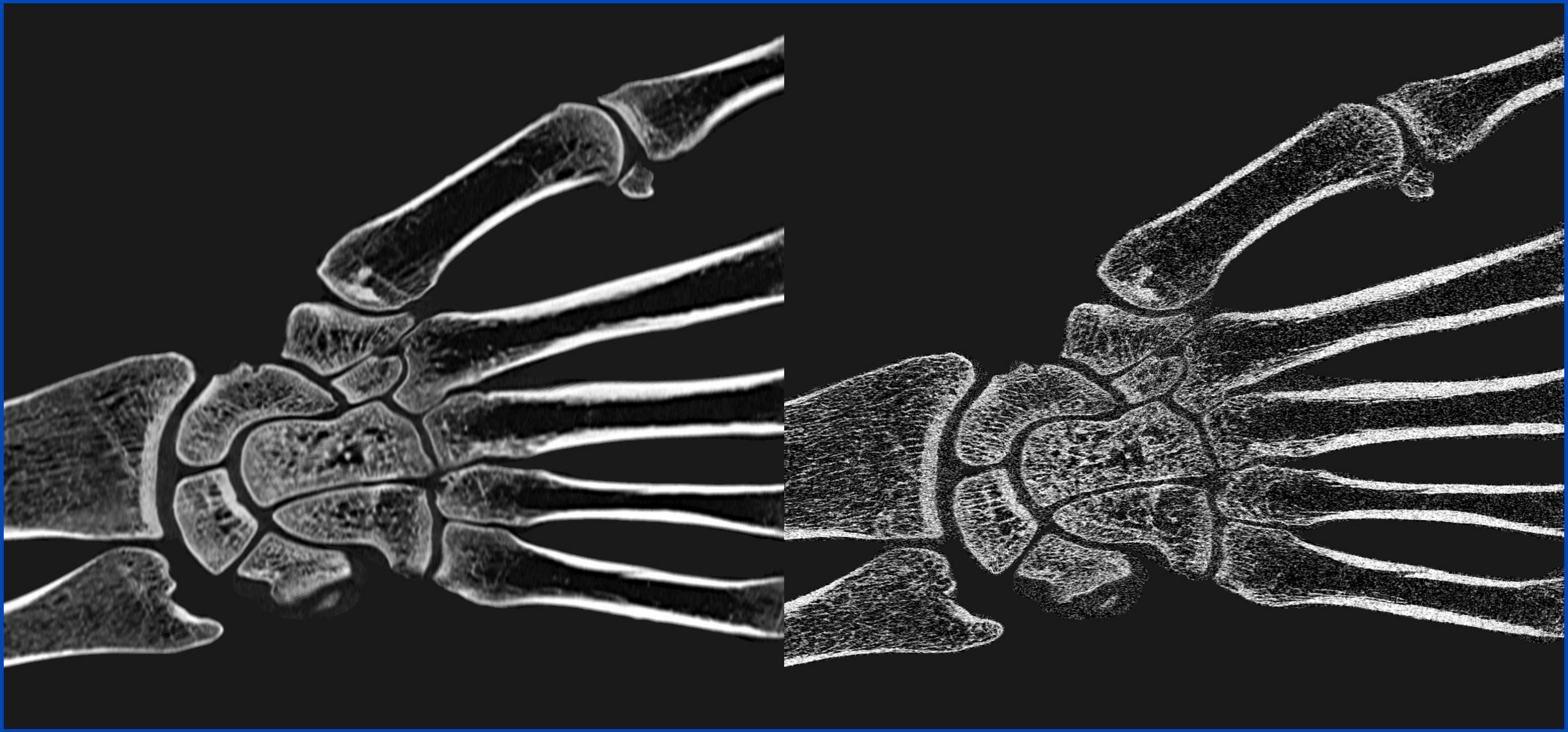

Reconstruction to mimick conventional energy-integrating CT, e.g. Somatom Flash

Reconstruction of data scanned at photon-counting CT Naoetom Alpha

Photon-Counting enables Visualization of Small Details

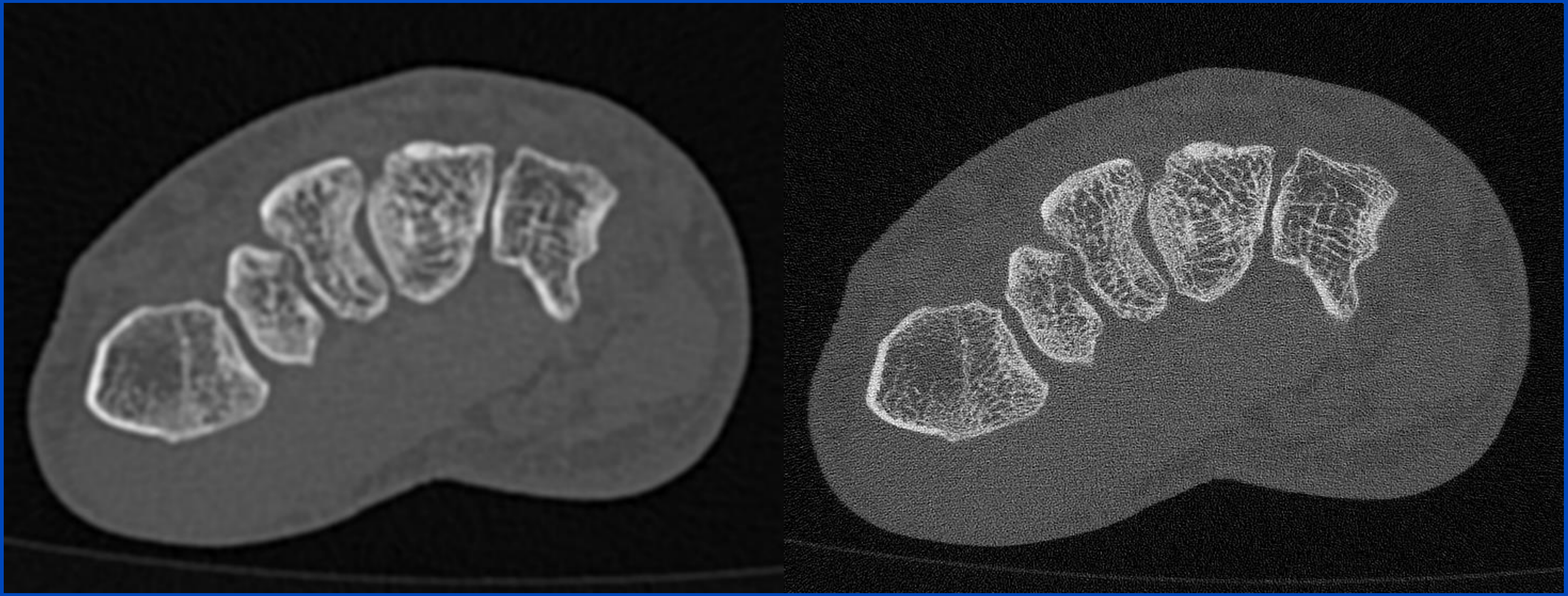

Reconstruction to mimick conventional energy-integrating CT, e.g. Somaton Flash

Reconstruction of data scanned at photon-counting CT Naoetom Alpha

SIEMENS Healthineers

dkfz.

Properties of Photon-Counting Detectors

- **Smaller detector pixels**
  - can deliver ultra high resolution imaging
  - less dose due for conventional spatial resolution[1] (“small pixel effect”)
- **No electronic noise**
  - advanced image quality in obese patients and low-dose scans
- **No downweighting of lower energy quanta**
  - improved image contrast
  - less dose due to increased iodine CNR[2] (“iodine effect”)
- **Intrinsic spectral sensitivy**
  - established dual energy applications available in any scan

[1] Klein, Kachelrieß, Sawall et al. “Effects of Detector Sampling on Noise Reduction in Clinical Photon-Counting Whole-Body Computed Tomography.” *Investigative Radiology* vol. 55(2): 111-119, 2020.
[2] Sawall, Kachelrieß et al. “Iodine Contrast-to-Noise Ratio Improvement at Unit Dose and Contrast Media Volume Reduction in Whole-Body Photon-counting CT.” *European journal of radiology* vol. 126: 108909, 2020.

Energy-Integrating vs. Photon-Counting Detectors

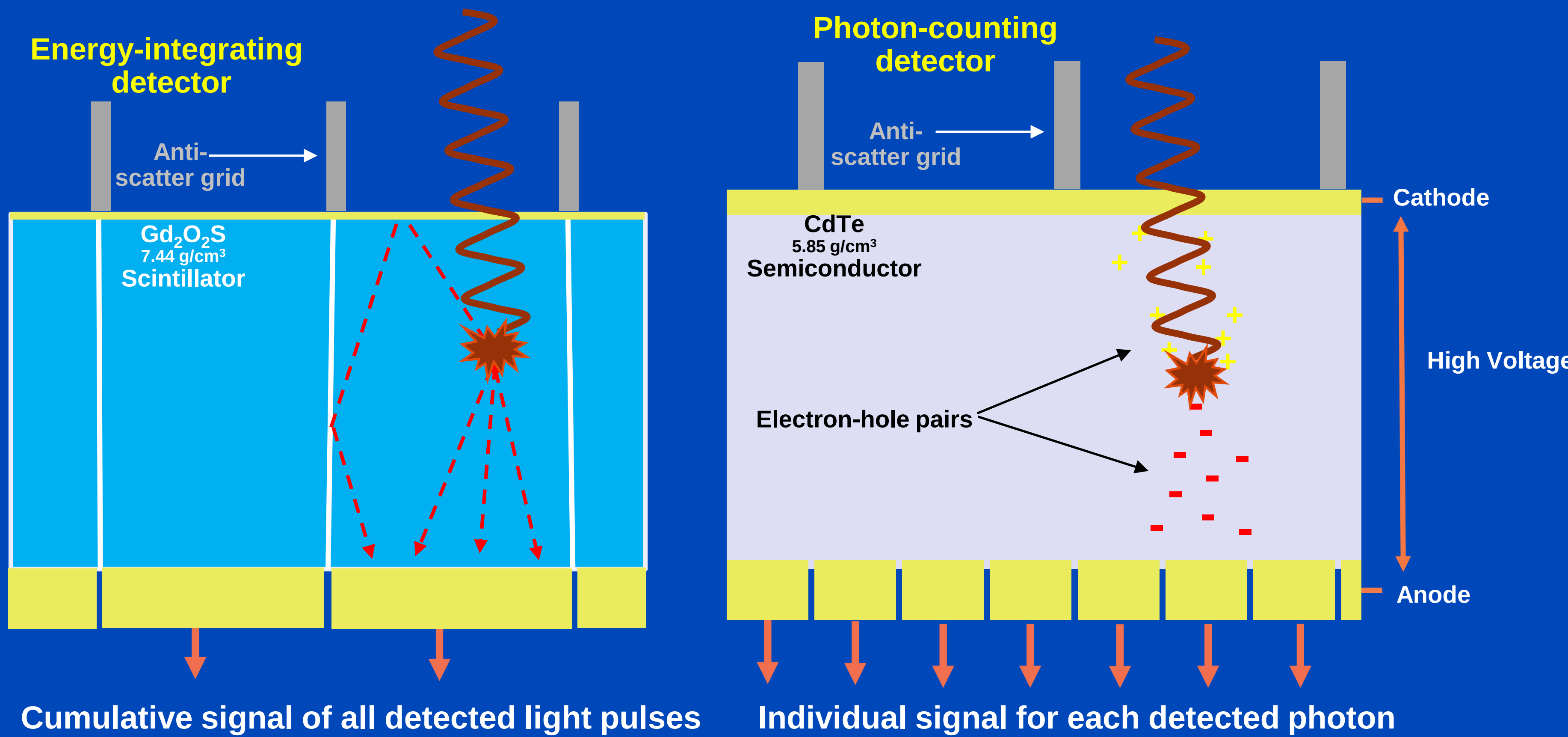

Photon-counting detector has several subpixels between lamellae of ASG

Scatter for Coarse ASG

Energy-integrating detector

Conventional ASG
Each pixel surrounded by ASG

Photon-counting detector

Coarse ASG
Several subpixel surrounded by ASG

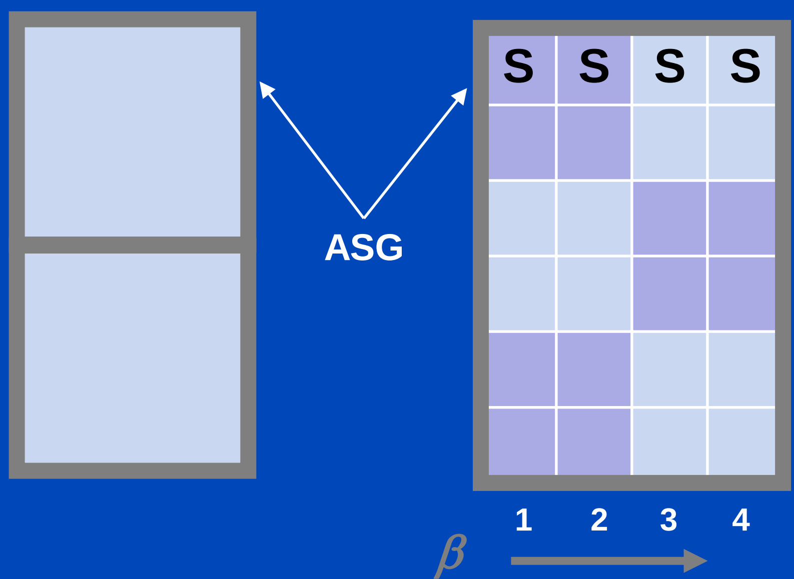

Primary radiation
Scatter measured by the detector
Scatter attenuated by the ASG

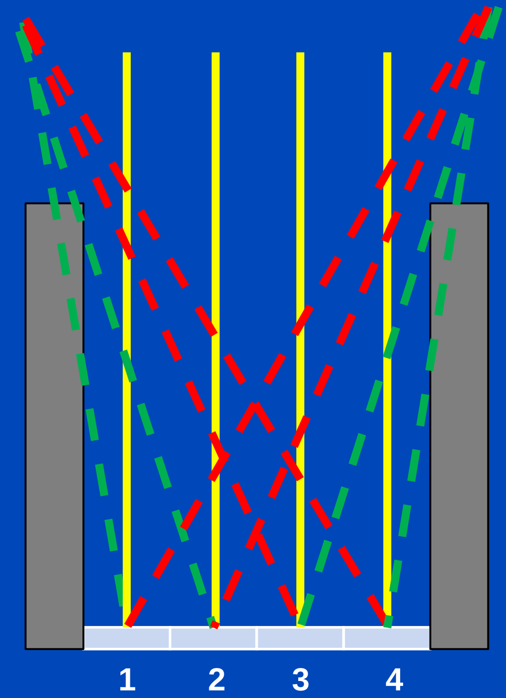

Coarse ASG leads to changing scatter intensity between neighboring pixel depending on the incident angle of the photon

Scatter for Coarse ASG

Four subpixel (S) merged to one macropixel (M)

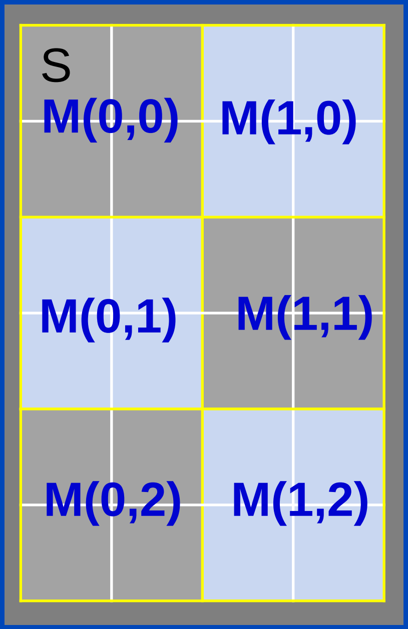

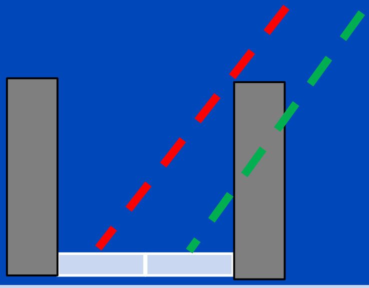

Scatter distribution averaged over all detector rows

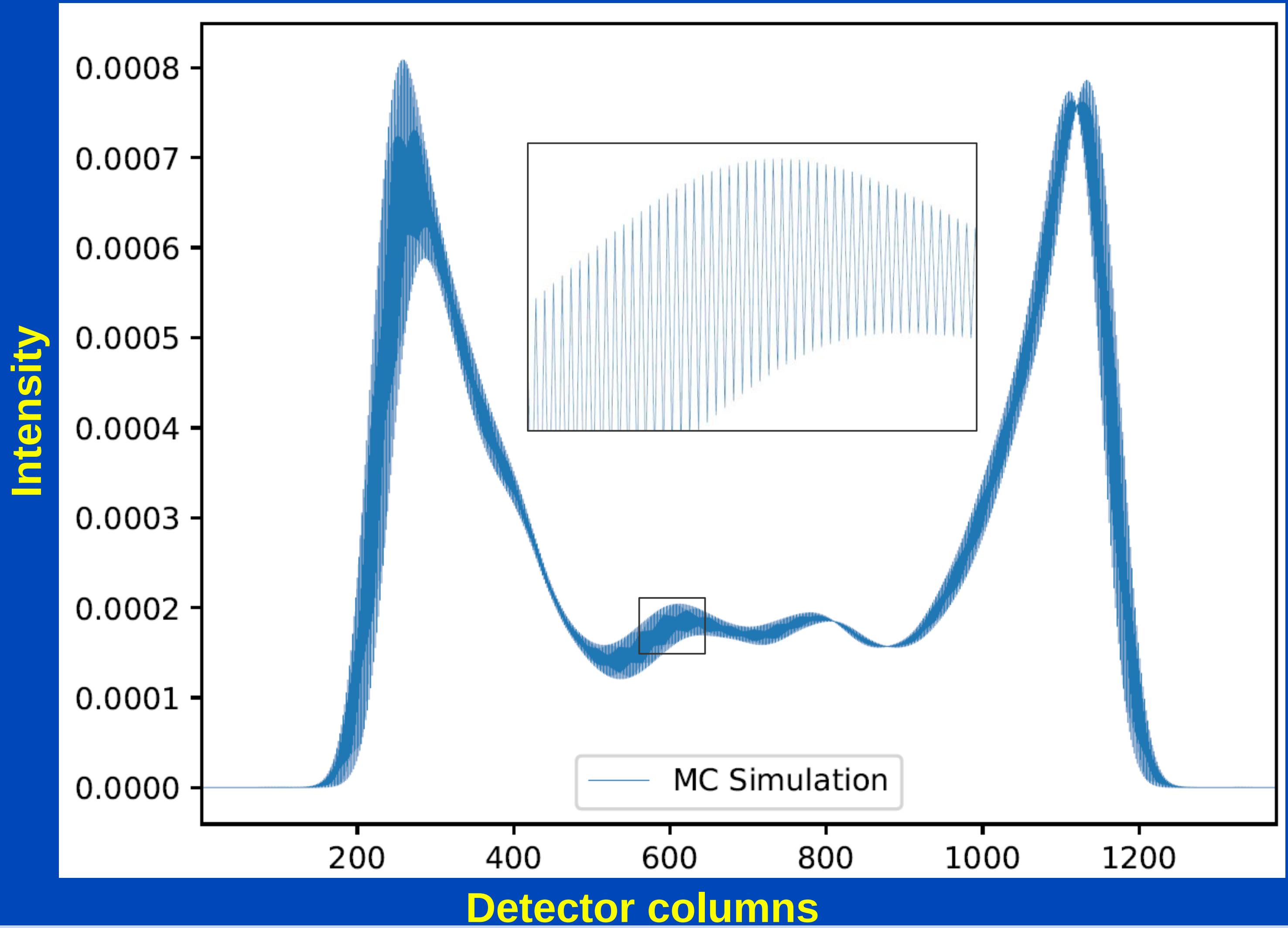

Scatter for Coarse ASG

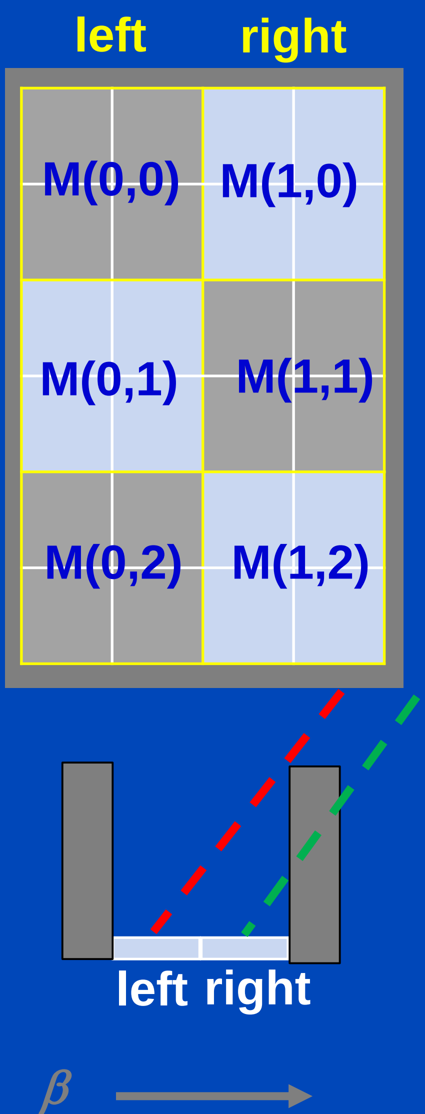

Scatter distribution averaged over all detector rows

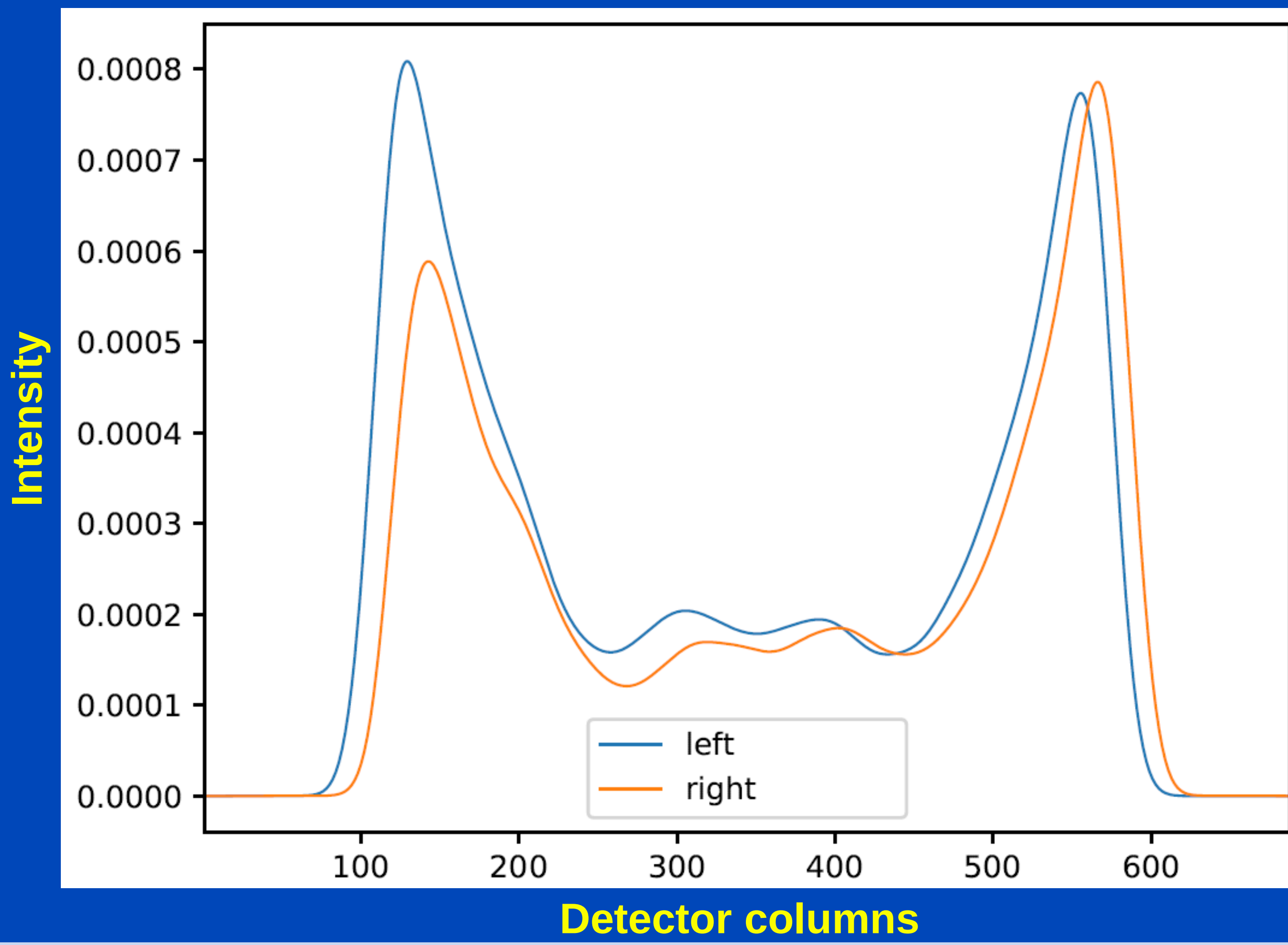

Scatter for Coarse ASG

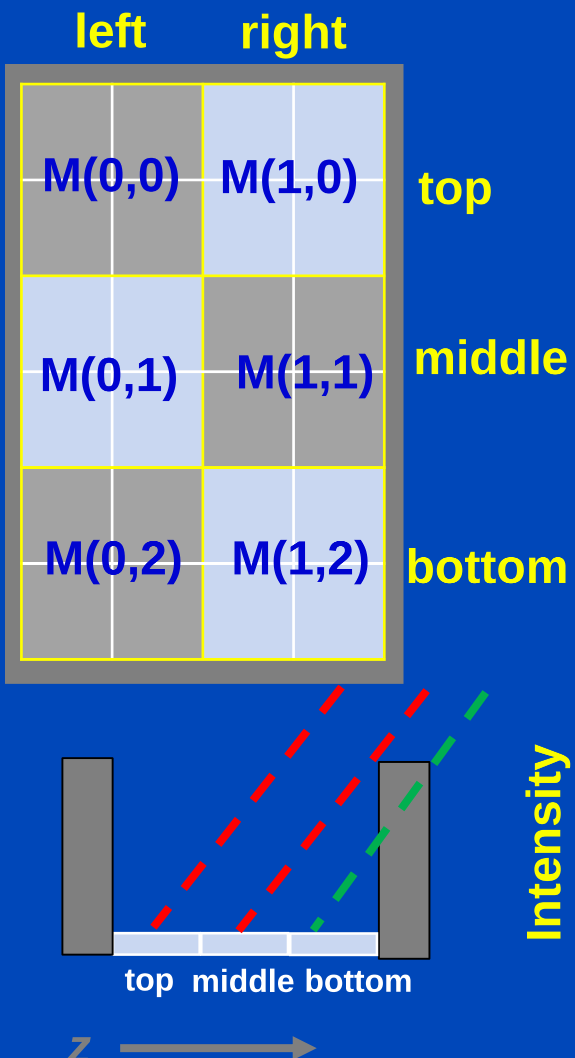

Scatter distribution over center detector column

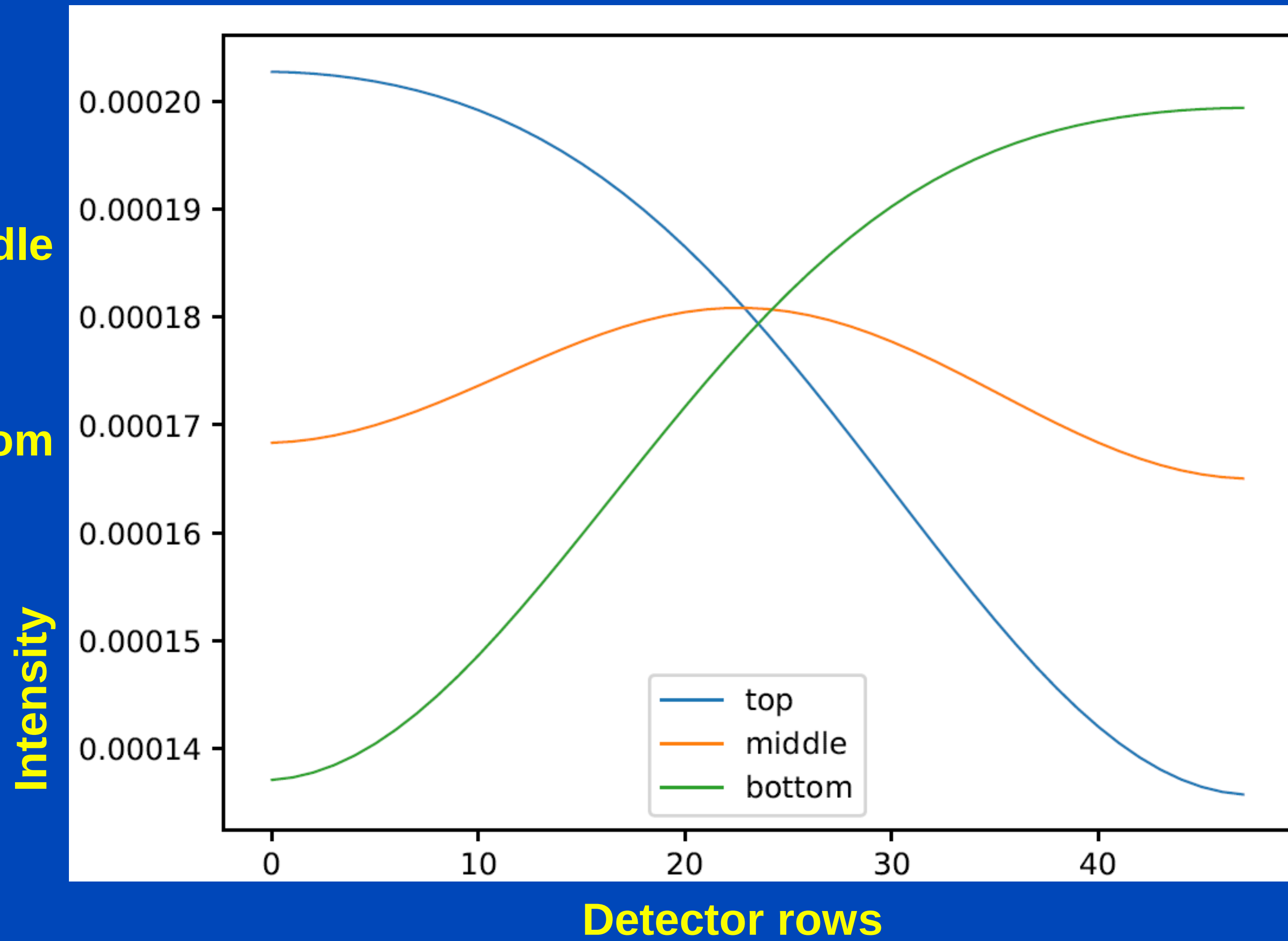

Scatter Artifacts of Coarse ASG

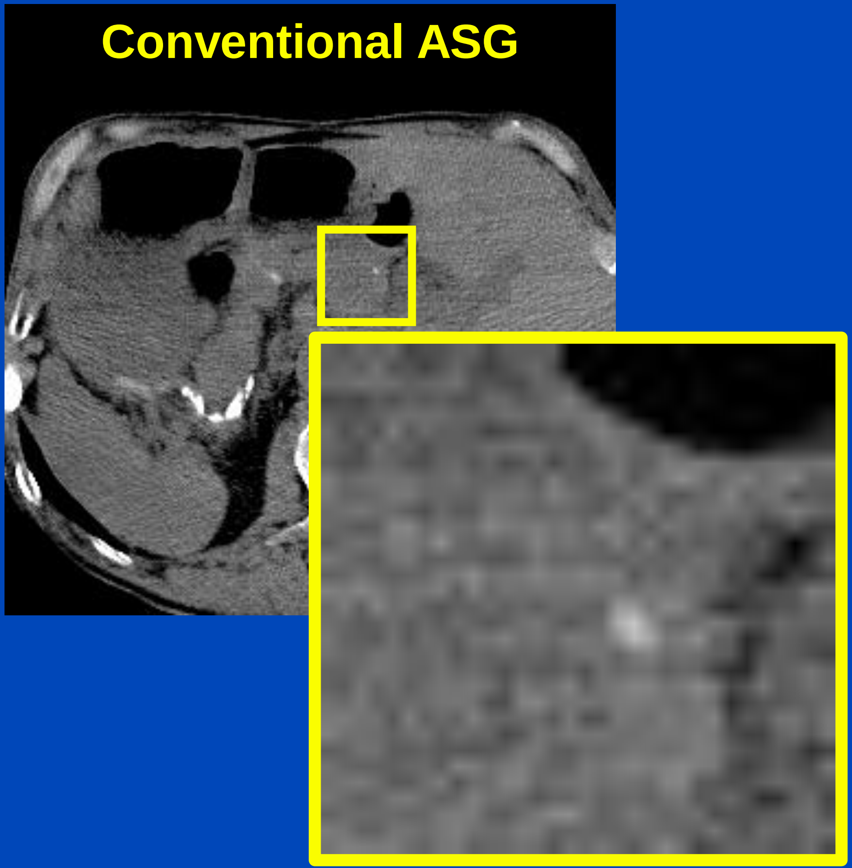

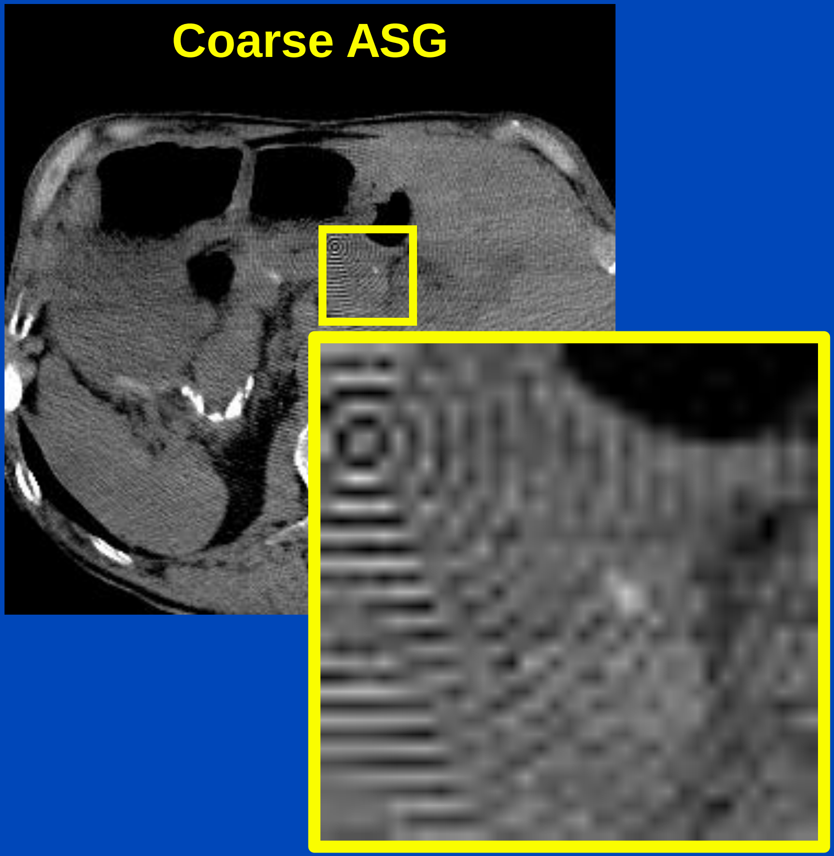

Coarse ASG can lead to scatter-induced moiré artifacts.

Reconstruction: C = 40 HU, W = 300 HU

Deep Scatter Estimation (DSE)

- Use a deep convolutional neural network to estimate scatter using the acquired projection data as input.[1,2]
- Train the network to predict Monte Carlo scatter estimates based on the acquired projection data.[1,2]
- DSE outperforms other scatter estimation techniques.[1,2,4,5]
- DSE is much faster than the Monte Carlo simulation.[1,2,5]
- DSE can also be trained with measured scatter data.[3]
- DSE shows great potential to correct for cross-scatter in dual source CT.[4,5]

Scatter profile from Monte Carlo simulation

Time: 65 s per projection = 14 h per circle scan

Scatter prediction from deep scatter estimation

Time: 3.3 ms per projection = 4 s per circle scan

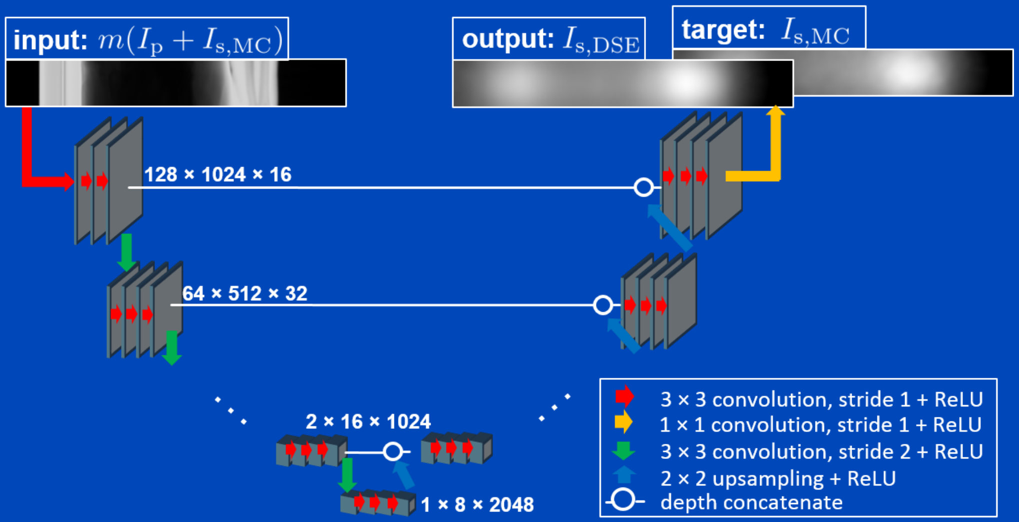

[1] J. Maier, M. Kachelrieß et al. "Deep Scatter Estimation (DSE)", SPIE 2017 and J. of Nondest. Eval. 37:57, July 2018.
[2] J. Maier, M. Kachelrieß et al. "Robustness of DSE", Med. Phys. 46(1):238-249, January 2019.
[3] J. Erath, M. Kachelrieß et al "Monte-Carlo-Free Deep Scatter Estimation (DSE) for X-Ray CT and CBCT", RSNA 2019
[4] J. Erath, T. Vöth, J. Maier, E. Fournié, M. Petersilka, K. Stierstorfer, and M. Kachelrieß, "Deep Scatter Correction in DSCT", CT Meeting August 2020.
[5] J. Erath, T. Vöth, J. Maier, E. Fournié, M. Petersilka, K. Stierstorfer, and M. Kachelrieß, "Deep Learning-Based Forward and Cross-Scatter Correction in DS CT" Med. Phys. 2021

Training and Validation Data

- **Monte Carlo simulation with the geometry of the photon counting CT scanner NAEOTOM Alpha (Siemens Healthineers)**
- **12 patients for training and 4 for validation**
- **14 z-positions with 36 projections each simulated for each patient**
- **8064 paired scatter and primary data pairs**
- **Simulation of coarse ASG with macro pixel with detector dimension of 1376 × 144 pixels**
- **6 different macro pixels locations**
- **Smooth only across same macro-pixel locations**

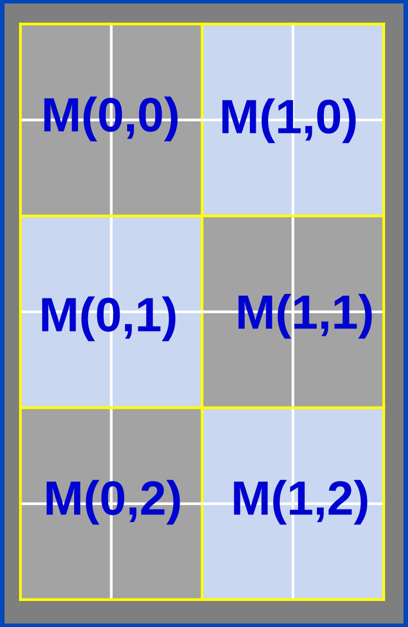

14 z positions

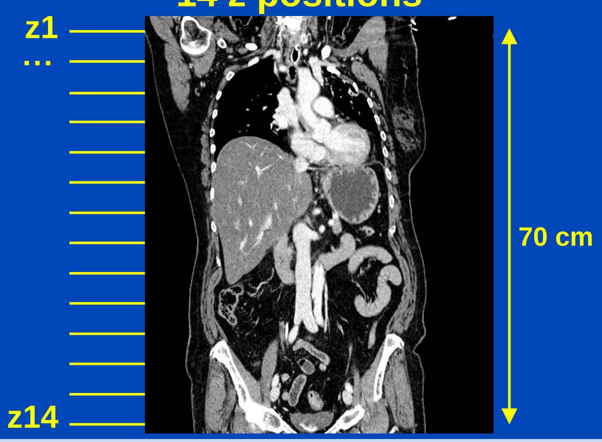

Training and validation patients with high variety and different clinical situations, important to consider scatter-to-primary ratio

Example of validation data set:

Network Architecture

Detector dimension
1376×144
Input mapping

$$p = -\ln\left(\frac{I_{\text{primary}}}{I_0} + \frac{I_{\text{scatter}}}{I_0}\right)$$

Each channel corresponds to a different pixel position between the lamallea of the ASG

Merging 6 different channels to obtain total scatter correction term

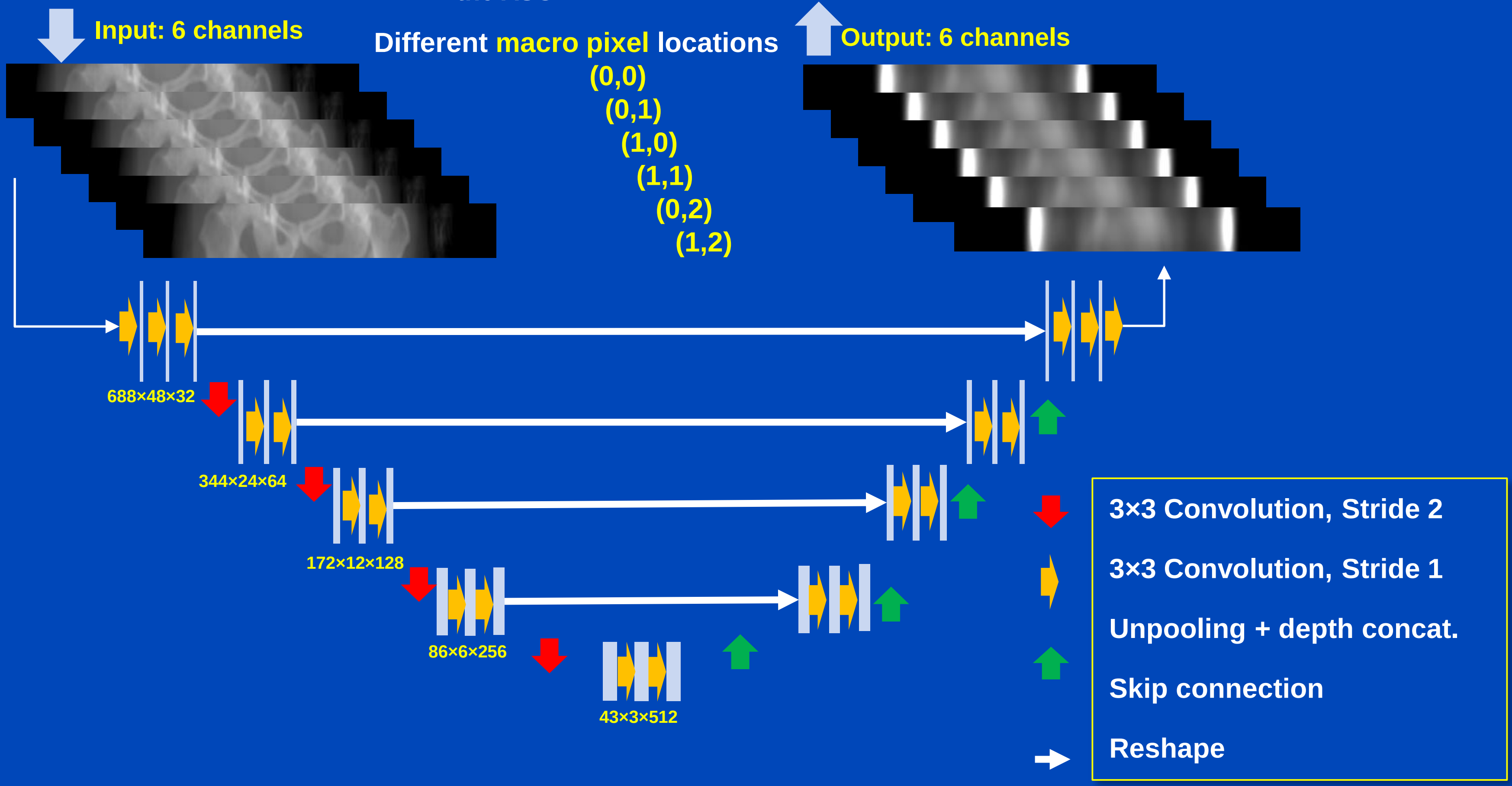

Predicton of Scatter Intensity

Scatter distribution of left and right columns averaged over all detector rows

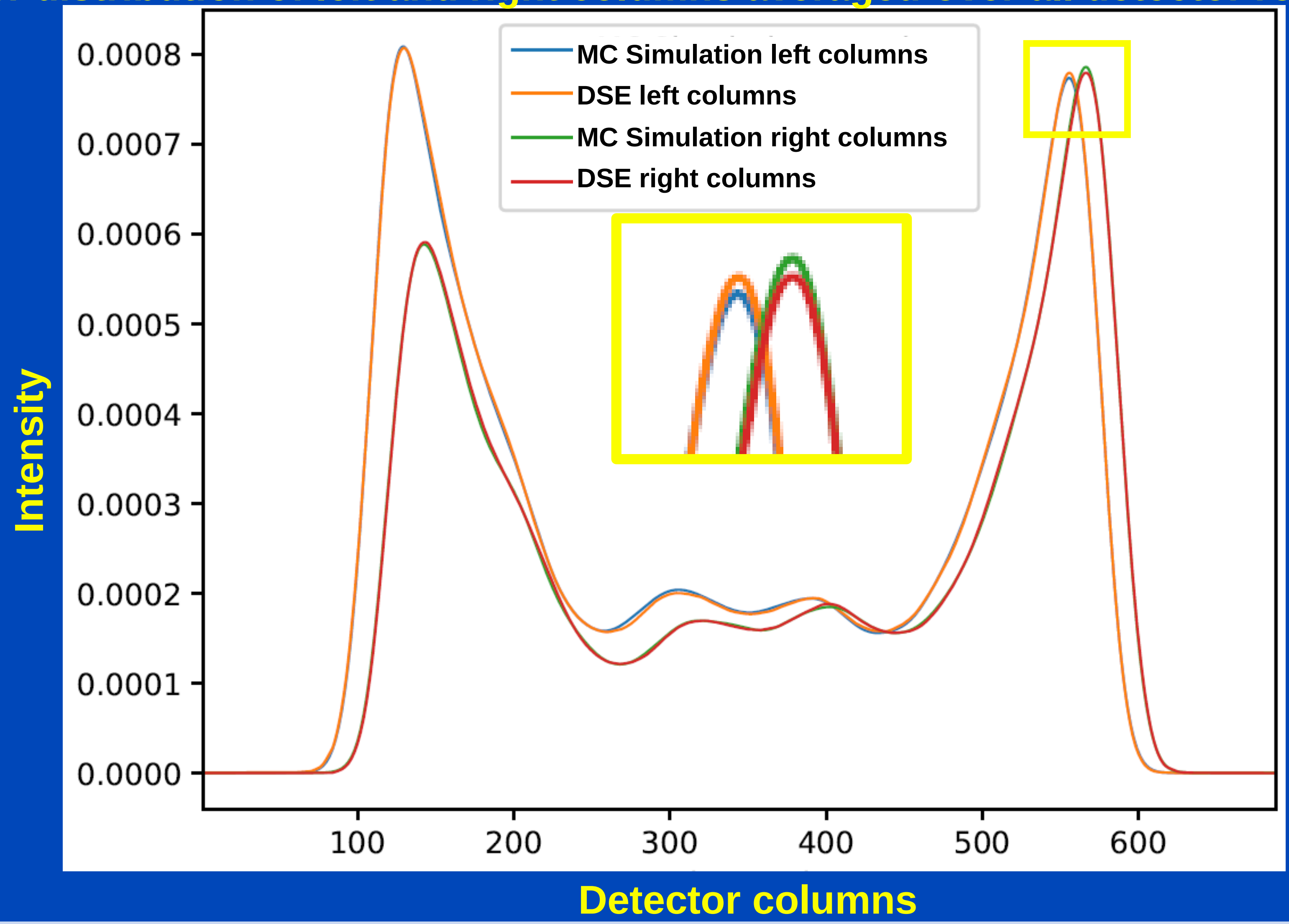

SIEMENS Healthineers

dkfz.

Results in Reconstructed Images

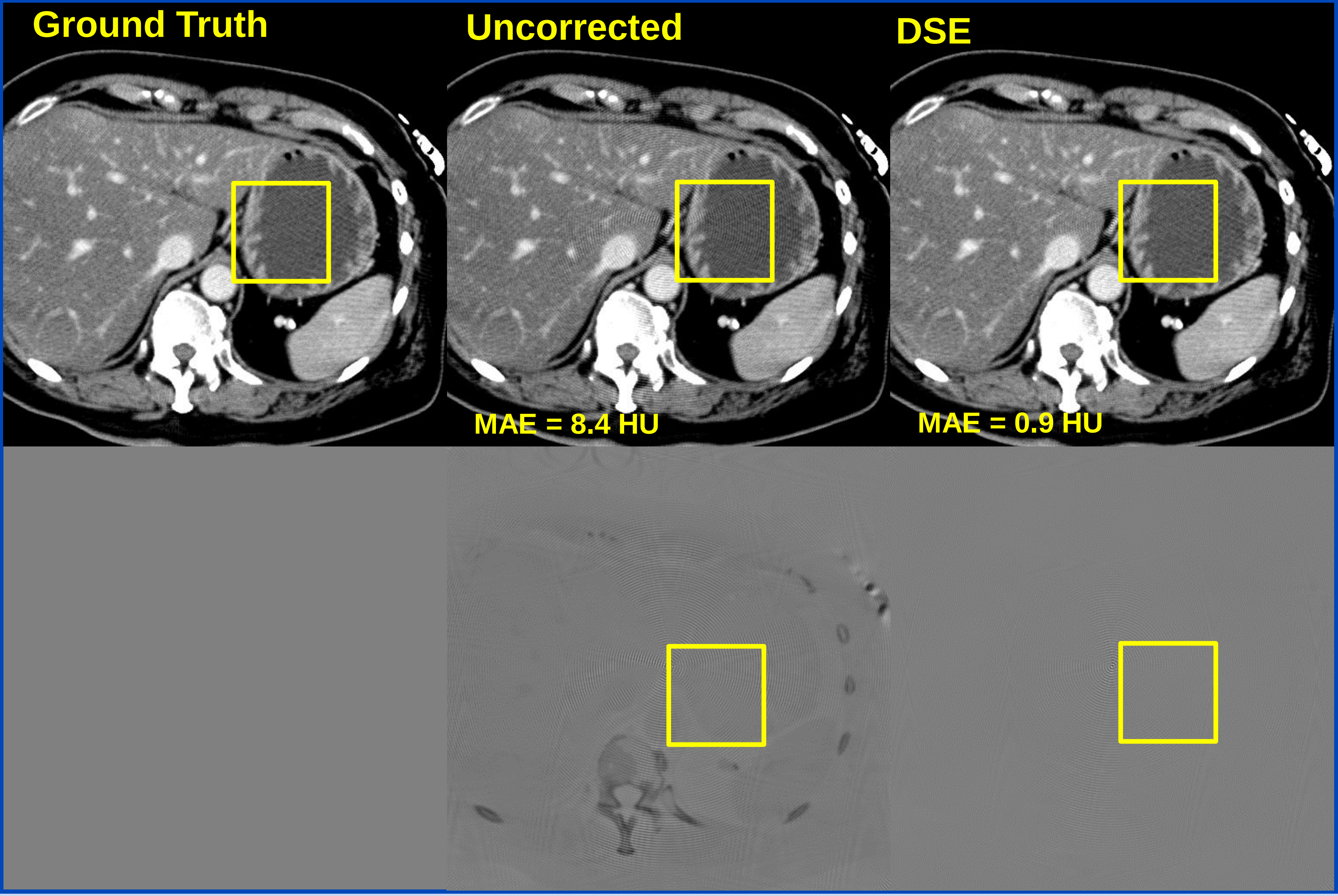

Simulated Reconstruction C = 0 HU, W = 400 HU,
Difference to GT C = 0 HU, W = 50 HU

Results in Reconstructed Images

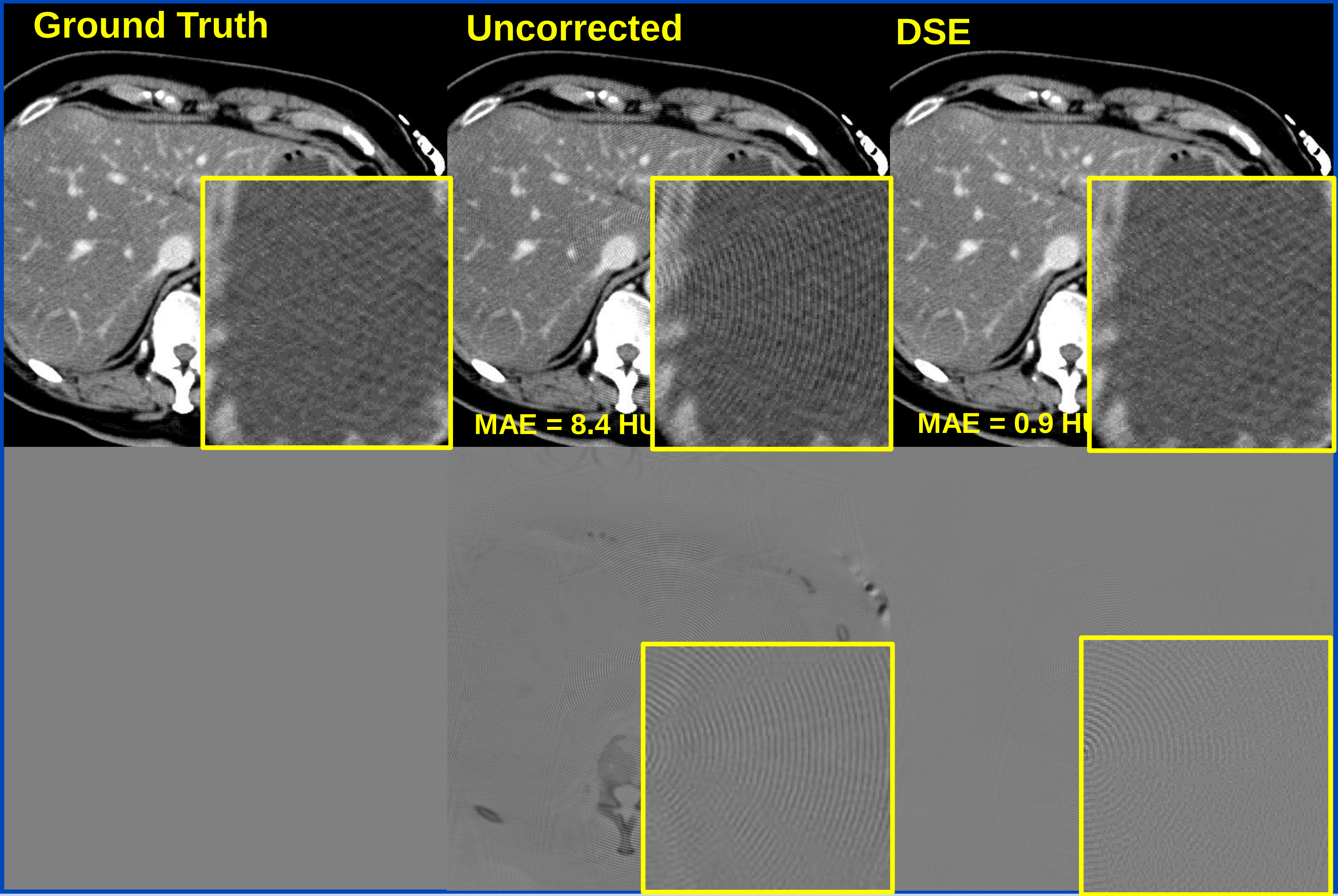

Simulated Reconstruction C = 0 HU, W = 400 HU,
Difference to GT C = 0 HU, W = 50 HU

Results in Reconstructed Images

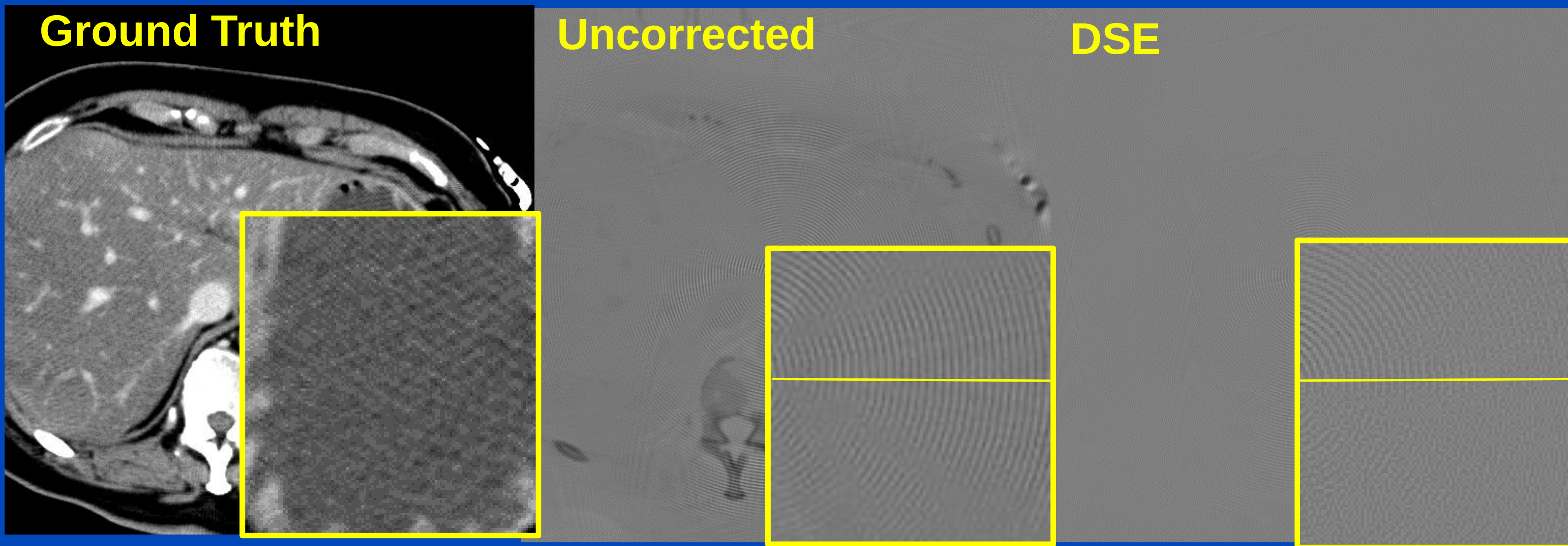

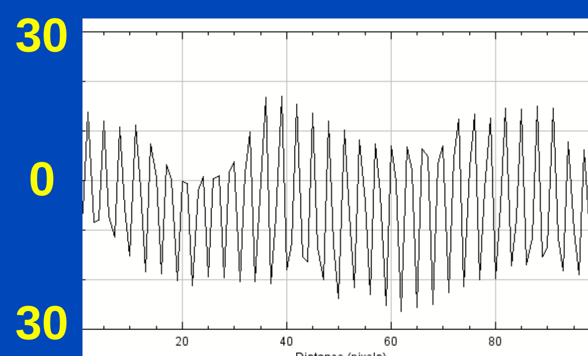

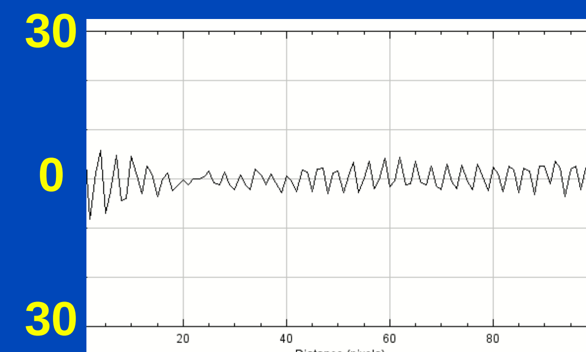

Amplitude of the moiré effect gets corrected from 30 HU to less than 5 HU.

SIEMENS Healthineers

Simulated Reconstruction *C* = 0 HU, *W* = 400 HU,
Difference to GT *C* = 0 HU, *W* = 50 HU

dkfz.

Results in Reconstructed Images

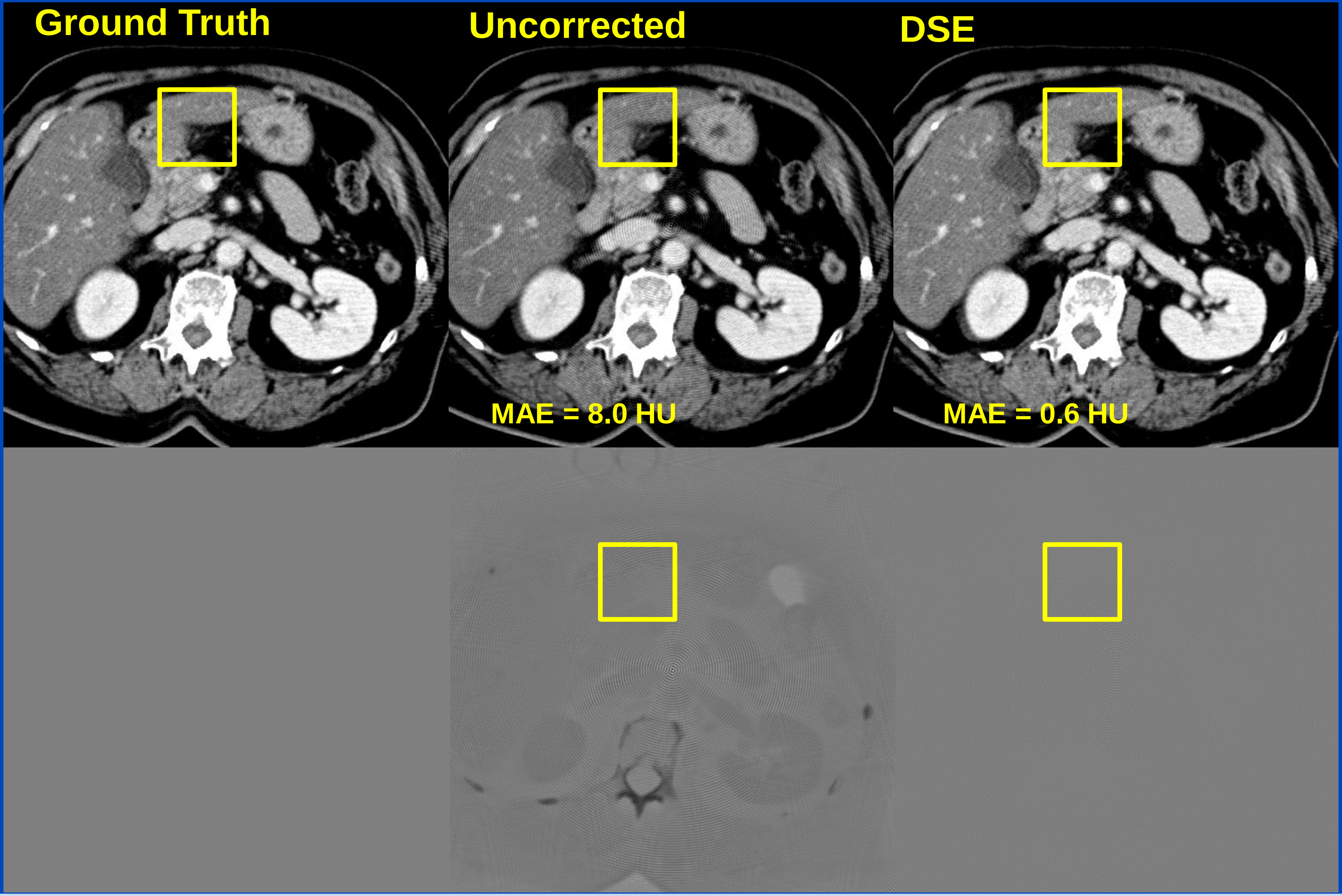

Simulated Reconstruction *C* = 0 HU, *W* = 400 HU,
Difference to GT *C* = 0 HU, *W* = 50 HU

Results in Reconstructed Images

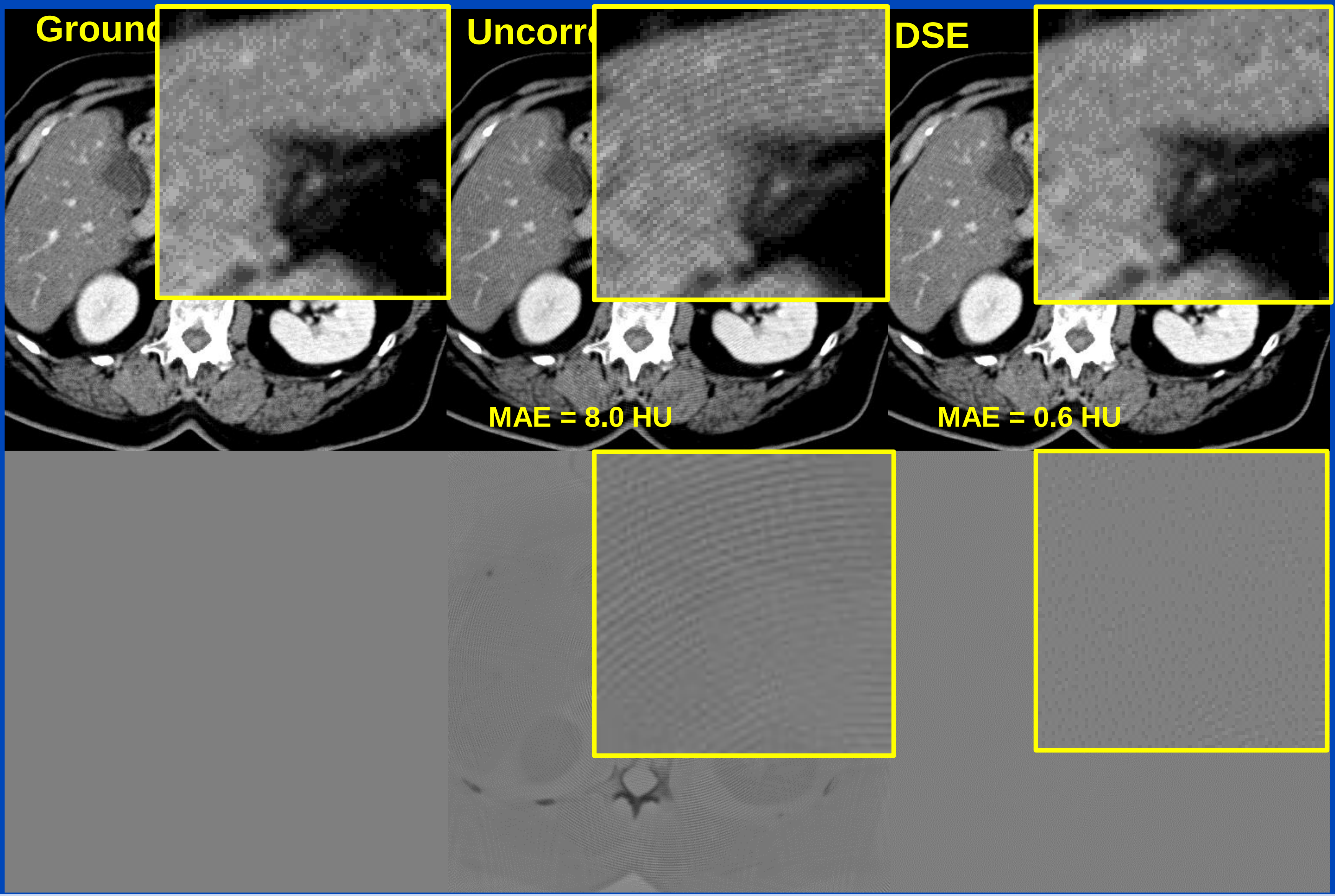

Simulated Reconstruction C = 0 HU, W = 400 HU,
Difference to GT C = 0 HU, W = 50 HU

Conclusions

- Smaller detector pixel and coarse anti-scatter grid can lead to moiré artifacts.
- Scatter induced moiré effect can be clearly corrected with deep learning-based scatter correction.
- With the proposed algorithm the mean absolute error (MAE) could be reduced from uncorrected about 9 HU to under 1 HU.
- The amplitude of the scatter induced moiré effect can be corrected from 30 HU to less than 5 HU.
- Next step: apply deep-learning based correction for measurements.

This presentation will soon be available at www.dkfz.de/ct.
Job opportunities through DKFZ's international PhD or Postdoctoral Fellowship programs (marc.kachelriess@dkfz.de).